Islamic University Journal of Applied Sciences (IUJAS)
https://journals.iu.edu.sa/jesc
Special Issue, February 2026, Pages 127-135
https://igee.univ-boumerdes.dz/ncaeee25/

Modeling of Grounding Grids under Lightning Currents Using a Nonuniform Transmission Line Approach

Boutadjine Ahmed [1,*]

[1] Department of Electrical Engineering-University of Jijel, Algeria, boutadjine92@gmail.com

*Corresponding author: (Boutadjine Ahmed), *Email Address*: boutadjine92@gmail.com

Abstract

Modeling a grounding system in the time domain makes it possible to account for the nonlinear phenomenon of soil ionization, which occurs following the injection of a very high-intensity lightning current. Several numerical studies using the Finite-Difference Time-Domain (FDTD) method have focused on modeling grounding systems while considering soil ionization. These works, which have produced excellent agreement with experimental measurements, directly solve Maxwell's equations in three dimensions (3D), but they remain computationally intensive and numerically complex. In this paper, we propose a model for a grounding grid that offers a simplified implementation while accounting for the various electromagnetic couplings that arise after spatial discretization of the grid, as well as for soil ionization caused by the injection of a high-intensity lightning pulse. This new formulation is developed based on the equations of nonuniform Transmission Lines (nuTL) combined with the Finite-Difference Time-Domain (FDTD) method.

Keywords: Modeling; Grounding Grid; FDTD; Ionization; nuTL.

https://doi.org/10.63070/jesc.2026.011
Received 24 November 2025; Revised 18 January 2026; Accepted 26 January 2026.
Available online 31 January 2026.
Published by Islamic University of Madinah on behalf of *Islamic University Journal of Applied Sciences*.
This is an open access article published under the Creative Commons Attribution 4.0 International license (CC BY 4.0): https://creativecommons.org/licenses/by/4.0/

1. Introduction

Lightning strikes are among the main causes of overvoltages and equipment failures in power transmission networks. When a direct lightning stroke impacts a transmission tower, the associated transient current propagates toward the grounding system. If the grounding is properly designed, it can effectively limit the Ground Potential Rise (GPR) and thereby prevent back-flashover phenomena [1]. To minimize such incidents, engineers must give particular attention to the correct dimensioning and configuration of grounding systems.

The design of an effective grounding system can be approached through three complementary methods : experimental, analytical, and numerical. Although experimental tests are indispensable [2], they are often insufficient to ensure reliable and reproducible results due to the heterogeneous nature of soils-characterized by stratification and large variations in resistivity. To complement experimental investigations, researchers increasingly rely on simulation methods based on [1] circuit theory, transmission line modeling and numerical resolution of Maxwell's equations. During the injection of a very high-intensity lightning current, the soil may experience significant heating, sometimes leading to ionization phenomenon [3]. To model this nonlinear behavior, several studies have been conducted. Among these different works, Liew's dynamic model is the one that comes closest to reality [4].

In this work, we aim to simplify the simulation of the transient behavior of a grounding grid while incorporating the effects of soil ionization. We propose a new numerical modeling approach developed in the time domain, based on the resolution of nonuniform transmission line equations using the Finite-Difference Time-Domain (FDTD) method [5]. This approach offers the advantage of being both very low computational time and straightforward to implement, while maintaining good accuracy in reproducing the electromagnetic coupling and ionization phenomena observed during high-intensity lightning strikes.

2. New formalism based on non-uniform transmission line theory

The use of numerical method FDTD requires the spatial discretization of the thin-wire conductor in element of size Δx. If the thin-wire conductor is considered as a transmission line and its discretization is achieved by neglect the propagation, then each element (cell) of size Δx is represented by the π electrical (Figure 1) circuit and the general equations for a cell ¨i¨ are given by telegrapher's equations as follows [6] :

$$\frac{\partial V(x_i,t)}{\partial x} + R_{ii} I(x_i,t) + M_{ii} \frac{\partial I(x_i,t)}{\partial t} = 0 \qquad (1)$$

$$\frac{\partial I(x_i,t)}{\partial x} + G_{ii}\, V(x_i,t) + C_{ii}\frac{\partial V(x_i,t)}{\partial t} = 0 \qquad (2)$$

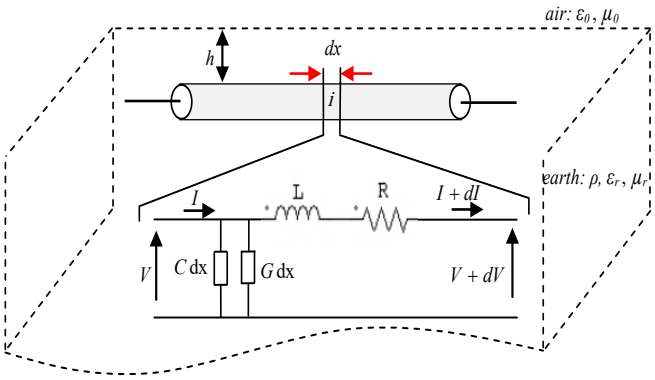


Figure 1. Equivalent electrical circuit of a cell.

These two partial differential equations describe the evolution of voltage $\boldsymbol{V(x_i,t)}$ and current $\boldsymbol{I(x_i,t)}$ as a function of distance ¨x¨ and time ¨t¨. In which appear $\boldsymbol{R_{ii}}$, $\boldsymbol{M_{ii}}$, $\boldsymbol{G_{ii}}$ and $\boldsymbol{C_{ii}}$ are respectively, the per unit length longitudinal resistance, longitudinal inductance, conductance to ground and capacitance to ground of a cell ¨i¨.

Classically, if we model an electrical device as thin-wire by adopting the transmission line approach, after subdivision of the conductor into several π-cells, equations (1) and (2) do not allow to take into account the electromagnetic interactions between two different cells (¨i¨ and ¨j¨) (Figure 2).

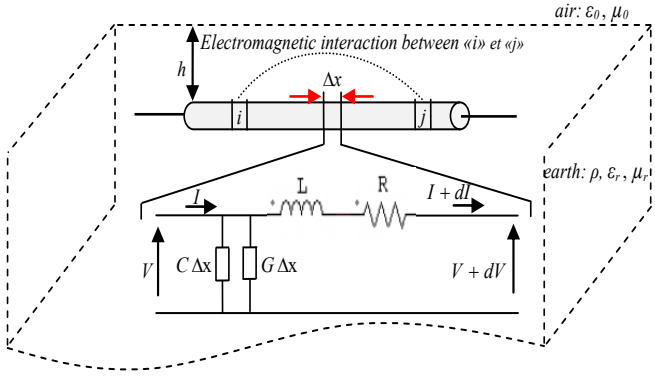


Figure 2. Electromagnetic interactions between cells ¨i¨ and ¨j¨.

So in our work, to take into account the electromagnetic interactions between two different cells ¨i¨ and ¨j¨ we complete the general and classical equations of transmission line (1) an d (2) as follow [5]:

$$\frac{\partial V(x_i,t)}{\partial x} + R_{ii} I(x_i,t) + \sum_{j=1}^{k_{max}} M_{ii}\frac{\partial I(x_i,t)}{\partial t} = 0 \qquad (3)$$

$$\frac{\partial I(x_i,t)}{\partial x} + G_{ii}\, V(x_i,t) + \sum_{j=1,j\neq i}^{k_{max}} G_{ij}\left[V(x_j,t) - V(x_i,t)\right] + C_{ii}\frac{\partial V(x_i,t)}{\partial t} + \sum_{j=1,j\neq i}^{k_{max}} C_{ij}\frac{\partial\left[V(x_j,t)-V(x_i,t)\right]}{\partial t} = 0 \qquad (4)$$

We calculate the self and mutual per-unit length parameters in (3) and (4) according to the geometrical position of the elements (cells) [7]. We therefore use in this paper rather the term nonuniform Transmission Line (nuTL) [5]. Note that, after subdividing the electrode into k_{max} cells of size Δx, the per unit length parameters matrix ([R], [L], and [G]) are calculated using the model proposed by Y. Liu [7]. Also, when the line is discretized into elementary segments (cells), we note the presence of a set of elementary electrical charges and the calculation of the matrix of the capacitance coefficients [CN] must be done by inverting the matrix of susceptance coefficient [P] [7].

$$[CN] = [P]^{-1} \tag{5}$$

The elements of the capacity matrix $[C]$ are then calculated as follows : $C_{ii} = CN_{ii}$, $C_{ij} = -CN_{ij}$ and $C_{ij} = C_{ji}$.

To apply the numerical method called FDTD [6] for solving the equations (3) and (4) along the line, we subdivide the grounding electrode into cells of length Δx and we place nodal voltages at its two ends and at its middle point (node) a branch (node) current (Figure 3). In the time domain, two adjacent current and voltage nodes are separated by $\Delta x/2$ in space and shifted by $\Delta t/2$ in time. Spatio-temporal discretization obeys a stability criterion [8].

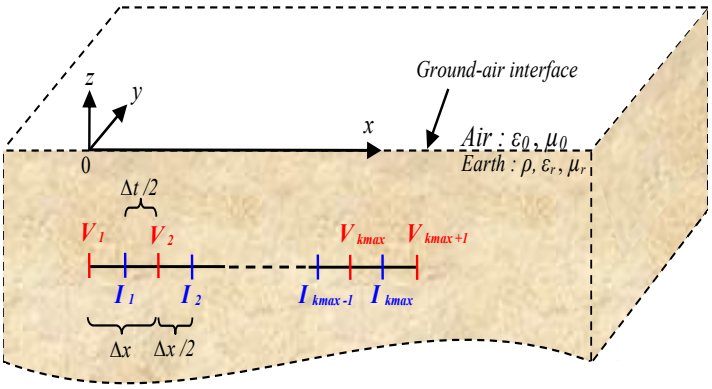


Figure 3. Presentation of nodal voltages and currents after spatial discretization of the buried conductor.

$$\frac{V_{i+1}^{n}-V_{i}^{n}}{\Delta x} + R_{ii}\frac{I_{i}^{n+1/2}+I_{i}^{n-1/2}}{2} + \sum_{j=1}^{k_{max}} M_{ij}\frac{I_{j}^{n+1/2}-I_{j}^{n-1/2}}{\Delta t} = 0 \tag{6}$$

$$\frac{I_{i}^{n-1/2}-I_{i-1}^{n-1/2}}{\Delta x} + G_{ii}\frac{V_{k}^{n}+V_{k}^{n-1}}{2} + \sum_{j=1,j\neq i}^{k_{max}} G_{ij}\frac{\left[\left(V_{j}^{n}-V_{i}^{n}\right)+\left(V_{j}^{n-1}-V_{i}^{n-1}\right)\right]}{2} + C_{ii}\frac{V_{k}^{n}-V_{k}^{n-1}}{\Delta t} + \sum_{j=1,j\neq i}^{k_{max}} C_{ij}\frac{\left[\left(V_{j}^{n}-V_{i}^{n}\right)-\left(V_{j}^{n-1}-V_{i}^{n-1}\right)\right]}{\Delta t} = 0 \tag{7}$$

Where ¨n¨ indicating time and ¨i¨ and ¨j¨ the space.

The objective of our work is to propose a new numerical model for studying the transient behavior of grounding grid.

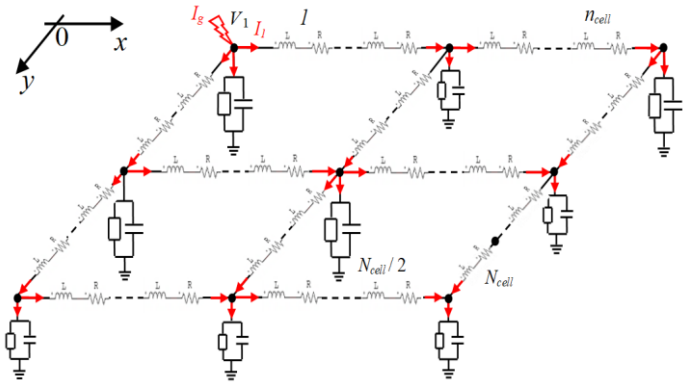


Figure 4. Electrical circuit equivalent of grounding grid.

For the grounding grid (Figure 4), the grid is subdivided into several π-shaped cells, each with a length Δx along the x-direction and a length Δy along the y-direction, assuming $\Delta x = \Delta y$.

- The intersections between the conductors represent the nodal tensions (physical nodes);
- The nodes located between two physical nodes represent a succession of branch currents and node voltages (fictitious nodes);

This new topological electromagnetic modeling consists on using the equations (6) and (7) to deduce a matrix system :

$$[A][X] = [B] \qquad (8)$$

The unknown vector [X] represents the nodal voltages in each node of the grounding grid and the currents of branches between two successive nodes after its subdivision. To generate the matrix system (8) in time, firstly we define the unknown vector as follows :

$$[X(t)] = \left[V_1(t), V_2(t), \dots, V_i(t), \dots, V_{k_{max}+1}(t), I_1(t), I_2(t), \dots, I_i(t), \dots, I_{k_{max}}(t)\right]^t \qquad (9)$$

Note that, the number of nodes ¨$k_{max} + 1$¨ for the voltages and the number of nodes ¨ k_{max} ¨ for the currents is given just for a single electrode. Also for the computer implementation, we shift the currents backwards by half a time step. Once the unknown vector is defined, to build the matrix [A] we apply the equation (6) on all voltages nodes and equation (7) on each of the current node.

[A] is a topological matrix defined from the per unit length parameters, the step Δx and the step Δt and [B] is source vector (contains the current source located at the injection point, and the known prior values of current and voltage). The matrix [A] is full and contains the couplings between cells which appear following the effects of mutual inductances, mutual capacitances and mutual conductances. This new writing (equations (6) and (7)) allows us to get as close as possible to full wave modeling using method of moment [1]. A certain advantage, compared to other purely numerical modeling, is to allow access to the currents and voltages at each time step.

3. Dynamic model of soil ionization in our modeling

Measurement results clearly show that under the effect of a strong discharge, a phenomenon of non-linearity appears in the soil [3]. In fact, when the leakage current intensity in soil is very high (ie $E \geq E_C, E$: the local electric field in the soil and E_C : the critical electric field of the soil), the zones around the grounding grid are going through an ionization and discharge. A dynamic model for taking into account the heating of the ground and the non-linearity of its resistivity in the presence of very intense currents was introduced by Liew [4] and compared to the measured results [9]. The dynamic model of Liew [4] is described by a closed cycle of three phases. During the first phase (phase 1), the resistivity of the soil remains constant, then the ionization phase (phase 2) occurs when the electric field in the soil is greater than its critical field ($E \geq E_C$), and finally the deionization phase (phase 3) when the electric field E in the region of the ionized soil drops below critical field E_c (Figure 5).

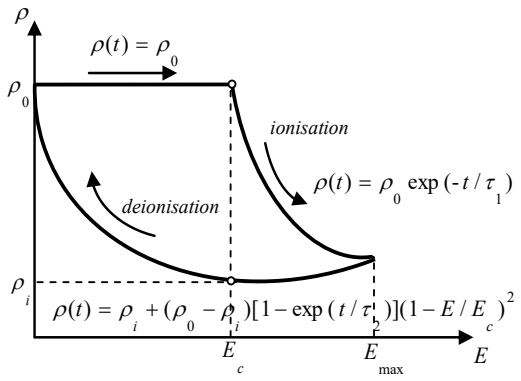


Figure 5. Resistivity profile in the dynamic model proposed by A. C. Liew [4].

For phases 2 and 3 of the dynamic cycle Liew [4] proposes analytical expressions to describe the variation of soil resistivity over time. Knowing that our temporal modeling allows us to calculate simultaneously at each time step both voltages, currents along the grounding grid and the leakage current in soil, in our work we easily apply the Liew model [4].

Indeed, we can introduce into our modeling the dynamic model of Liew [4] knowing that we can know the electric field (E) in the near of the grounding grid by applying Ohm's law (10) :

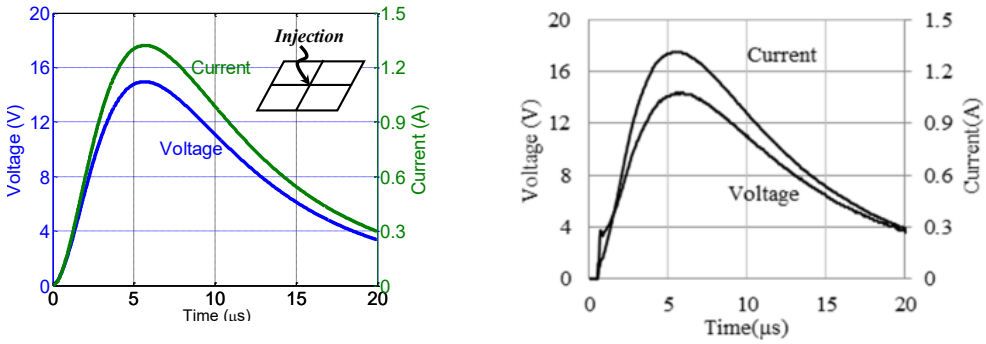
$$J_l = \sigma E = \frac{1}{\rho} E \qquad (10)$$

With : $J_l = \frac{I_l}{S}$ and $S = 2r\pi\Delta l$

Where J_l is the surface density of the leakage current in the soil, I_l is the leakage current in the soil (transversal current drained to earth), S is the lateral surface of a cell, Δl is the length of cell after spatial discretization of the buried grid and r is the radius of the buried electrodes composing the grounding grid.

4. Simulation results

Firstly, we validate our proposed modeling approach; we precede by a comparison of our calculation results with those obtained by the measurement carried out by N. Harid [2]. For this application, we consider the case of square grounding grid ($3m \times 3m$) buried at a depth $d = 0.3\ m$ in a soil with two horizontal layers. The first layer has a depth of 8 meters and has electrical resistivity $\rho_1 = 200\ \Omega.m$. The second layer with infinite depth and has electrical resistivity $\rho_2 = 50\ \Omega.m$. For our calculations we use the notion of apparent electrical resistivity [10] for taking into account the two-layer soil.



(a) Our calculations results (b) Measured results [2]

Figure 6. GPR at the injection point current of the grounding grid.

Figure 6 shows the variation of the Ground Potential Rise (GPR) at the injection point current. We note a perfect agreement between our calculations (Figure 6 (a)) and those measured (Figure 6 (b)) [2]. To complete the study of the effect of soil ionization on the transient response of grounding systems with complex geometries, we consider the case illustrated in Figure 7. It consists of a square-shaped grounding grid buried in a homogeneous soil characterized by an electrical resistivity of $\rho = 200\ \Omega.m$, a relative permittivity of $\varepsilon_r = 10$, and a critical electric field value of $E_C = 200\ kV/m$.

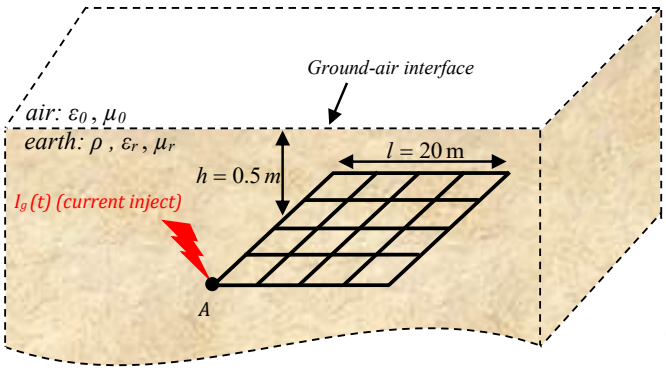


Figure 7. Grounding grid with corner injection (point A).

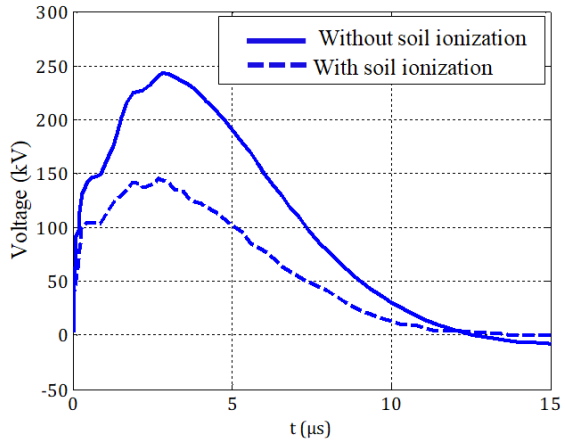


Figure 8. Voltage at point A of grounding grid.

The results presented in Figure 8 clearly show that the occurrence of the ionization phenomenon (ie $E \geq E_C$) leads to a decrease in the Ground Potential Rise (GPR) (with a reduction of the peak voltage by nearly 40%) since the electrical resistivity of the soil in the vicinity of the grounding conductors decreases up to the maximum value of the electric field (E_{max}) in the soil (see Figure 5). We then observe a reverse phenomenon, in which the soil begins to recover its initial electrical resistivity (de-ionization phase), and the GPR subsequently follows the same process. The adopted modeling approach makes it possible to identify the region of the soil, in the vicinity of the conductors, that is affected by ionization. The computation times for this application (for a transient of 15 μs) are low and are given in Table 1 (using a processor : Intel® Core™ i7 - 4600U CPU at 2.10 GHz).

Table 1. CPU time consumed.

	Without soil ionzation	With soil ionization
CPU time (sec)	312.044	345.15

5. Conclusion

The good results obtained when considering soil ionization confirm that the proposed model, developed from the nonuniform transmission line equations and the FDTD numerical method, is well suited for taking into account the dynamic behavior of soil resistivity during the injection of very high current amplitudes. Since the computation times are quite reasonable and the quality of the results is satisfactory, the proposed

References

[1] Ametani Akihiro, and al., Guideline for Numerical Electromagnetic Analysis Method, CIGRE Technical Brochure 543, pp. 1-106. 2013.

[2] N. Harid and al., On the Analysis of Impulse Test Results on Grounding Systems, EEE Transactions on Industry Applications, 2015.

[3] A. Mousa, The soil ionization gradient associated with discharge of high currents into concentrated electrodes, IEEE Transactions on Power Delivery, Volume: 9, Issue: 3. 1994.

[4] A. C. Liew and al., Dynamic model of impulse characteristic of concentrated earths, Proc. IEE, 121, (2), pp. 123–135. 1974.

[5] A. Boutadjine, B. Nekhoul and al., Realistic modeling of the grounding system transient behavior with frequency dependence, Electric Power Systems Research, volume 203, February 2022, 107644.

[6] C. R. Paul, Analysis of Multiconductor Transmission Lines, John Wiley & Sons, Inc., New York, 1994.

[7] Y. Liu, N. Theethayi, and R. Thottappillil, An Engineering Model for Transient Analysis of Groundig system Under Lightning Strikes: Nonuniform Transmission-Line Approach. IEEE Trans. on Power Delivery. Vol. 20. N° 2. April 2005.

[8] D. M. Sullivan, Electromagnetic Simulation Using the FDTD Method, by Wiley edition. 2013.

[9] K. Otani and al., FDTD Simulation of Grounding Electrodes Considering Soil Ionization, International Conference on Lightning Protection (ICLP), Vienna, Austria. 2012.

[10] IEEE Guide for Measuring Earth Resistivity, Ground Impedance, and Earth Surface Potentials of a Grounding System. Revision of IEEE Std 81-1983.